Journal of Controlled Release 316 (2019) 1–11

Contents lists available at ScienceDirect

Journal of Controlled Release

journal homepage: www.elsevier.com/locate/jconrel

Transdermal finasteride delivery via powder-carrying microneedles with a diffusion enhancer to treat androgenetic alopecia

Suyong Kim[a], Jaehong Eum[a], Huisuk Yang[b], Hyungil Jung[a,b,*]

[a] Department of Biotechnology, Building 123, Yonsei University, 50 Yonsei-ro, Seodaemun-gu, Seoul 03722, Republic of Korea
[b] Juvic Inc., 272 Digital-ro, Guro-gu, Seoul 08389, Republic of Korea

ARTICLE INFO

Keywords:
Transdermal drug delivery
Dissolving microneedles
Lipophilic powder
Finasteride
Androgenetic alopecia

ABSTRACT

Androgenetic alopecia is a common form of scalp hair loss that affects men in their mid-twenties and increases with age. Finasteride (FNS) has been approved and used orally to treat androgenetic alopecia; however, systemic effects on other androgen-dependent tissues cause severe side-effects. To overcome these systemic effects and target hair follicles in the scalp only, numerous topical formulations of FNS have been developed and further combined with the solid microneedle (SMN) technique to create micro-channels in the skin, thus overcoming the skin barrier properties. However, low delivery efficiency and concerns over patient safety of SMNs remain major limitations of the treatment. In the present study, we developed a novel FNS delivery system comprising powder-carrying microneedles (PCMs), which is a patch-less and self-administered powder delivery technique that simultaneously overcomes the safety issues. This system could directly implant FNS inside the skin by encapsulating the FNS powder in the center of the PCMs. In addition, we introduced the concept of a diffusion enhancer for this system, which facilitated the dissolution and release of the implanted FNS powder to achieve its successful intradermal delivery. Using implanted FNS powder as a reservoir inside the skin, this novel system permitted sustained release of the implanted FNS powder for 3 days with only one application of FNS-PCMs. In addition, compared with the topical FNS-gel, the developed system showed a higher efficacy in promoting hair growth and increased the amount and density of hair while addressing the safety concerns. This approach has the potential to advance the field of transdermal drug delivery for any type of powdered drug in a wide variety of biomedical applications.

1. Introduction

Androgenetic alopecia, also known as male-pattern baldness, is a common form of scalp hair loss that begins in men in their mid-twenties and increases with age [1]. The incidence of androgenetic alopecia is higher in men than in women, because the hormone testosterone, which is converted to dihydrotestosterone by type-2 5α-reductase in hair follicles, plays a key role in male androgenetic alopecia [2,3]. High expression of dihydrotestosterone promotes shrinking and weakness of hair follicles; therefore, inhibitors of type-2 5α-reductase have been developed to prevent hair loss or to stabilize and maintain the density of newly acquired hair [4–6]. Finasteride (FNS), a synthetic inhibitor of type-2 5αreductase, has been approved and used orally to treat androgenetic alopecia [7,8]. Oral administration is the most preferred and convenient method because of good patient compliance. However, orally administered FNS has a systemic effect and causes severe side-effects on other androgen-dependent tissues, such as impaired reproductive function, impotence, erectile dysfunction, and gynecomastia [9,10].

To overcome these side-effects of oral administration, topical applications of FNS have been developed because the target tissue of FNS for androgenetic alopecia is restricted to the hair follicles in the scalp. Although oral administration of FNS is only approved by the Food and Drug Administration (FDA) and the European Medicines Agency (EMA) for the treatment of androgenetic alopecia currently, many researches have been focused on topical delivery of FNS due to its safety. Especially, various topical formulation techniques, such as permeation chemicals [11], liposomes [6,9,10], and nanoparticles [12] have been developed for the intradermal delivery of FNS to the reticular and hypodermic regions, which contain most of the hair follicles [13]. However, many of these formulations have poor penetration because the outermost skin layer, the stratum corneum, acts as a physical barrier to the entrance of substances into the skin. To overcome this hurdle in penetration, microneedle techniques that can pierce the skin physically

* Corresponding author at: Department of Biotechnology, Building 123, Yonsei University, 50 Yonsei-ro, Seodaemun-gu, Seoul 03722, Republic of Korea.
E-mail address: hijung@yonsei.ac.kr (H. Jung).

https://doi.org/10.1016/j.jconrel.2019.11.002
Received 1 August 2019; Received in revised form 27 October 2019; Accepted 1 November 2019
Available online 02 November 2019
0168-3659/

have been introduced [14,15].

Previously, solid microneedles (SMNs), made of metal or silicon, were used to create micro-channels in the skin [16,17]. After the application of SMNs, topical formulations could be delivered via these channels, thus improving the delivery efficiency to hair follicles. However, SMNs also induce side-effects, such as irritation, redness, and red spots on the application site, which are caused by infection or exposure to air immediately after treatment [18]. In addition, SMNs are typically made of permanent materials, which form hazardous wastes, and raise concerns over patient safety and their inappropriate or accidental reuse [19]. Moreover, although this method promotes the absorption of the formulations, the delivery efficiency remains low because SMNs are used as an additive technology of the topical formulations [20]. Therefore, a new strategy to deliver FNS inside the skin directly is required to increase the delivery efficiency.

Recently, as an alternative to SMNs, dissolving microneedles (DMNs), which comprise polymeric micro-sized needles that release their loaded therapeutics into dermal layers after penetrating the skin, have been developed as an advanced transdermal drug delivery system [21–24]. Lacking the side-effects or safety issues of SMNs, DMNs also deliver therapeutics into the dermal regions directly; thus, FNS is considered one of the best candidates for the application of DMN technology. However, to date, most therapeutics delivered via DMNs have been limited to hydrophilic compounds because of the water-soluble nature of the backbone polymers use to achieve homogeneity or for the regular encapsulation of therapeutics [25,26]. Moreover, lipophilic drugs, such as FNS, aggregate or crystallize with the backbone polymers during the mixing step in the DMN fabrication process, making it difficult to fabricate DMNs; even if successfully fabricated, the encapsulated drugs cannot diffuse out of the DMNs inside the skin [26,27]. However, to the best of our knowledge, a strategy compromising intradermal delivery of FNS with effective permeation via DMNs, although desirable, has not been introduced.

In this study, we designed a novel FNS delivery system using powder-carrying microneedles (FNS-PCMs) with a topical diffusion enhancer (DE) to treat androgenetic alopecia. The FNS powder was encapsulated in the center of the DMN structure [28], which overcame the insolubility problem of the lipophilic drug in the conventional DMN fabrication process. By using the inherent microneedle function which overcomes the skin barrier properties, FNS powder was physically penetrated and implanted inside the skin. In addition, the topical application of DE, which is composed of similar solvent compositions of FNS-gel, was introduced sequentially on the application sites of FNS-PCMs to improve their dissolution and release of the implanted FNS powder. After the fabrication of FNS-PCMs, their physical properties and skin penetration ability were determined, and the efficacy of this novel DE-adapted application system was visualized qualitatively using Nile red as a model drug, and quantitatively using FNS in Franz diffusion cell test. Moreover, using C57BL/6 N mice, the amount of residual FNS was analyzed to indicate the clearance of the implanted FNS powder, which validated the safety of the method. Further, the hair growth promotion effect of the FNS-PCMs was compared with that of topically administered FNS-gel. The delivery of FNS via PCMs with DE offers a novel microneedle approach to treat androgenetic alopecia without any apparent safety issues.

2. Materials and methods

2.1. Fabrication of FNS-PCMs

A polydimethylsiloxane (PDMS) mold was created by casting 5 × 5 microneedle master structures with a height of 800 μm and a base diameter of 450 μm. A 10 % (w/v) carboxymethyl cellulose (CMC, Sigma-Aldrich, St. Louis, MO, USA) solution was prepared using a planetary centrifugal mixer (ARV-310; Thinky Corp., Tokyo, Japan) at 5,000 rpm for 10 min. Carboxymethyl cellulose was used as a backbone polymer of the FNS-PCMs because of its biodegradable, biocompatible, and viscous nature [29]. After casting 50 μL per cm^2 of CMC solution on the surface of the PDMS mold, the holes in the mold were filled under centrifugation at 5,000 rpm for 5 min. The solution was then dried at ambient temperature for 24 h, resulting in a solidified array with cavities in the center of the DMN structures, which was detached from the PDMS mold. The arrays were positioned in the holes of the fixing layer, and the protective layer was assembled by aligning the holes. The fixing layer had an array of holes to ensure that the DMNs are positioned and fixed exactly, and the protective layer with the same array of holes was used to physically protect the loaded powder from scattering. After loading the FNS powder (Sigma-Aldrich) in the holes of the protective layer, the two layers were centrifuged horizontally at 5,000 rpm for 5 min. After de-masking the protective layer, a second protective layer including a thin CMC film (thickness: 30 μm) was assembled. The micropillar arrays were then aligned with the holes of the second protective layer, resulting in the FNS-PCM implantation device [30]. For *in vitro* distribution analysis, the cavities were filled with Nile red powder (Sigma-Aldrich) as a model drug (Nile red-PCMs).

2.2. Fabrication of FNS-gel and DE

Among various topical formulations of FNS, a chitosan-based aqueous formulation was prepared as a control compared to this FNS-PCM/DE system, for high permeation of FNS in the reticular and hypodermic regions of the scalp [13]. Briefly, a solvent consisting of ethanol (99.5°, Sigma-Aldrich), propylene glycol (Sigma-Aldrich), and distilled water at a ratio of 55:5:38.75 (v/v) was mixed and vortexed. Then, 0.25 % (w/v) of FNS and 1 % (w/v) of chitosan (Sigma-Aldrich) were added, and homogenized sequentially at 5000 rpm for 10 min in the planetary centrifugal mixer. For the *in vitro* distribution analysis, Nile red was used instead of FNS (Nile red-gel). In addition, using the same solvent composition at a ratio of 60:10:38.75 (v/v), the DE was fabricated for the topical application on the FNS-PCM implantation sites to improve the dissolution and diffusion of the implanted FNS powder.

2.3. Morphologies, physical properties, and skin penetration analysis of FNS-PCMs

To validate the morphological properties of the FNS-PCM structures, the length and tip diameter were measured under a microscope (bright field, mode, M165FC, Leica, Wetzlar, Germany). In addition, to analyze the skin penetration ability, the mechanical fracture force of a single FNS-PCM structure was assessed using a displacement force machine (Z0.5 T N, Zwick/Roell Inc., Ulm, Germany) [31,32]. Briefly, after a single FNS-PCM structure was separated and attached to the stainless-steel station of the force machine, the axial force was recorded when the sensor probe was pressed onto the FNS-PCM in a downward vertical direction at a speed of 3.6 mm/min. To analyze the skin penetration ability, FNS-PCM arrays were applied on hair-removed pig cadaver skin (thickness: 800 μm, Cronex, Hwaseong, Korea). The perforations of the skin were stained with 0.4 % trypan blue solution (Sigma-Aldrich) for 30 min and then imaged under the microscope.

2.4. In vitro skin permeation and retention test

The *in vitro* skin permeation and retention test was conducted using a vertical-type Franz diffusion cell (Hanson, Chatsworth, CA, USA) with the pig cadaver skin. The test was conducted in quadruplicate with three groups: The FNS-gel group, the FNS-PCM group without DE (FNS-PCM only group), and the FNS-PCM group with DE (FNS-PCM/DE group). In the FNS-gel group, 10 μL per cm^2 of FNS gel was applied on the skin topically following the guidelines for *in vitro* application (OECD Test Guideline 428: Skin Absorption: *in vitro* Method, 2004). In the FNS-PCM only group, FNS-PCMs (at 25 microneedles per cm^2) were applied on the skin using the implantation device. In the FNS-PCM/DE group,

FNS-PCMs were applied and then 10 μL per cm^2 of DE was applied sequentially on the FNS-PCMs implantation site. The tissues of the groups were carefully mounted onto the donor compartment of the diffusion cell. The receptor chamber was filled with phosphate-buffered saline (Life Technologies, Eugene, OR, USA) with 20 % (v/v) ethanol, and maintained at 32 °C using a water jacket. After 24 h, 1 mL aliquots were withdrawn from the receptor and analyzed using high-performance liquid chromatography (HPLC).

The amount of FNS retained in the skin was determined after the permeation test. The FNS powder that did not diffuse out after DE treatment and thus remained inside the skin in a powdered state at the implantation sites was washed out several times using distilled water and the skin was gently dried using tissue paper. The skin was cut into small pieces using scissors, homogenized with 50 % (v/v) solution of methanol (Sigma-Aldrich) for 5 min, and sonicated in a water bath sonicator (Branson Ultrasonics Corp., Danbury, CT, USA) at 25 °C for 30 min. The solution was centrifuged at 5,000 rpm for 10 min, and the FNS content in the supernatant was determined using HPLC.

2.5. HPLC conditions for FNS

The quantitative determination of FNS was performed using a reverse-phase HPLC system (Waters 600S, Waters, Milford, MA, USA) with a C18 column (150 mm × 4.6 i.d., Cosmosil 5C18-AR-II, Nacalai Tesque Inc., Kyoto, Japan). A stock solution of FNS was serially diluted from 0 to 500 μg/mL ($R^2 \geq 0.99$) to prepare the calibration curve. The mobile phase comprised a mixture of acetonitrile:methanol:water (20:40:40). The phase remained isocratic and the flow rate was 1.0 mL/min. The detection wavelength for FNS was 210 nm, and the retention time was 13.5 min.

2.6. Qualitative distribution analysis of Nile red-PCMs and gel

The Nile red-gel group, the Nile red-PCM group without DE (Nile red-PCM only group) and the Nile red-PCM group with DE (Nile red-PCM/DE group) were analyzed for the distribution of Nile red in the skin qualitatively. After 24 h of Franz diffusion cell experiments, the Nile red powder remained inside the skin in a powdered state at the implantation sites was washed out several times using distilled water and the skin was gently dried using tissue paper. The skin surfaces (inner and outer surface of the skin) and cross-sections of the three groups were then photographed under the microscope (bright field and fluorescent mode) to confirm the lateral and vertical diffusion of Nile red.

2.7. In vitro diffusivity analysis of FNS by X-ray diffraction (XRD)

The diffusivity of FNS inside the skin was confirmed by XRD analysis performed on randomly oriented samples continuously scanned over the interval 10-60°, 2-theta using an high-resolution XRD (Ultima IV, Rigaku Corp., Tokyo, Japan) with Bragg-Brentano geometry (2-theta/theta) at 40 kV and 30 mA X-ray and K-beta filter radiation. For analyzing the diffusivity of FNS by DE *in vitro*, the pig cadaver skin after implantation of FNS-PCMs immediately was compared by the FNS-PCM only group and the FNS-PCM/DE group. For the sustained release of the implanted FNS powder for 3 days, the skin treated with daily application of DE after the permeation test was analyzed. After the permeation test of each group, all skin samples were dried at 32 °C for 1 day, and the implantation sites of FNS-PCMs were sectioned using scissors and attached to the station of the machine for the XRD analysis.

2.8. In vivo clearance test

All animal experiments were conducted according to procedures approved by Institutional Animal Care and Committee (IACUC) at Yonsei University. Healthy male C57BL/6 mice (7–8 weeks old, OrientBio, Seongnam, Korea) were used in this study. After being housed for 1 week for environmental adaptation, the dorsal skin was shaved using an electric clipper and depilated using hair-removal cream (thioglycolic acid 80 %, Viokox SA, Aldaia, Spain) 1 day before the test. About 0.5 g of the cream was applied on the hair-clipped back of the mice for 2 min, and the cream was wiped off using tissue paper for depilation. The back skin was rinsed extensively with distilled water to remove the remaining thioglycolic acid. The mice without significant wounds on their backs were selected and grouped randomly.

To assess the clearance of implanted FNS powder and validate its safety, after FNSPCMs implantation and immediately DE application at day 0, four groups were designed as follows: (a) Sacrifice at day 0; (b) Sacrifice at day 1; (c) additional DE application at day 1, and sacrifice at day 2; and (d) additional DE application at day 1 and 2, and sacrifice at day 3, and two groups as controls were additionally designed as follows: (e) without DE application at day 1, and sacrifice at day 2; (f) without DE application at day 2, and sacrifice at day 3 (n = 4 per group). On the end points of each group, the mice were sacrificed and the dorsal skin over the application site was sampled and cut into small pieces using scissors. The samples were homogenized with 50 % (v/v) solution of methanol, sonicated at 25 °C for 30 min, and centrifuged at 5000 rpm for 10 min. The content of FNS in the supernatant was analyzed using HPLC.

2.9. In vivo evaluation of hair growth promotion

To evaluate hair growth promotion, a control group (a non-treated group), an FNS-gel group, and an FNS-PCM/DE group were designed (n = 5 per group). In the FNS-gel group, 10 μL of FNS-gel was applied in 1 cm^2 of dorsal skin once a day. In the FNS-PCM/DE group, FNS-PCMs and sequential DE were applied into 1 cm^2 of dorsal skin, and then daily application of additional DE was conducted for 2 days (with the application of FNS-PCMs every 3 days). The applications of each group were continued for 12 days and the degree of hair growth was evaluated every 3 days by visual scoring of a hair growth quantification scale as follows: (0) initial state; (1) grey to black coloration; (2) short visible hair; (3) sparse long hair; (4) dense long hair; and (5) complete hair growth [33,34]. One week after the test, the dorsal skins of all groups were shaved using an electric clipper to analyze application and non-treated sites; the scalp was imaged using a portable scalp analysis machine (A-One Tab, Bomtech Electronics, Seoul, Korea). The area of the dense long hair of the FNS-PCM/DE group was measured using ImageJ software (NIH, Bethesda, MD, USA).

2.10. Storage conditions for a stability test

FNS powder, FNS-gel, and FNS-PCMs were sealed in Eppendorf tubes. After wrapping with aluminum foil, samples were stored for up to 8 weeks at 25 °C and 40 % relative humidity using a temperature regulator machine (Jeio Tech, Seoul, Korea). The FNS contents were measured at 0, 4, and 8 weeks using HPLC.

2.11. Statistical analysis

SPSS (IBM, Armonk, NY, USA) was used for the statistical analysis. Comparisons of the experimental and control groups were performed using one-way analysis of variance (ANOVA) followed by a *post-hoc* Scheffe test. Statistical significance was set as $p < 0.05$.

3. Results and discussion

3.1. Fabrication of FNS-PCMs

A schematic representation of the fabrication process of the FNS-PCMs is shown in Fig. 1. The process consisted of two steps: fabrication of DMN arrays with cavities and loading the FNS powder into the

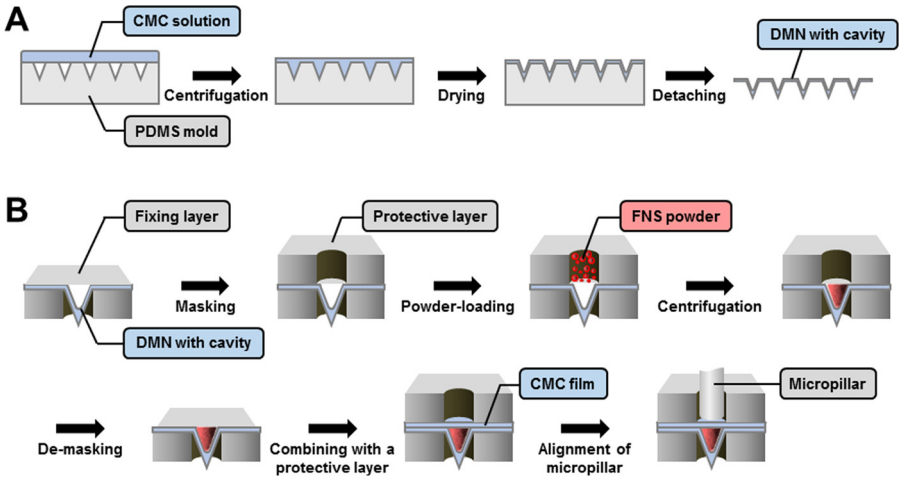

Fig. 1. Schematic representation of the fabrication process of finasteride (FNS)-loaded powder-carrying microneedles (FNS-PCMs). (A) Using a polydimethylsiloxane (PDMS) mold, a carboxymethyl cellulose (CMC) solution was cast, dried, and detached, resulting in a solidified array with cavities in the center of the dissolving microneedle (DMN) structures. (B) The arrays were assembled in the holes of a fixing layer, and masked with a protective layer. Then, the FNS powder was loaded into the holes of the protective layer, and the two layers were centrifuged to load the powder into the cavities. After de-masking the protective layer and assembly with a new protective layer coated with a CMC film, the micropillar arrays were aligned with the holes, resulting in the FNS-PCM implantation device.

cavities. In the first step, the DMN arrays with cavities were prepared using a mold-casting method [35]. Briefly, arrays of 5 × 5 microneedle master structures were fabricated from stainless-steel using laser cutting, and then an inverse mold was created by casting the master structures in PDMS. After filling a CMC solution into the arrays of microneedle-shaped holes of the PDMS mold by centrifugation, drying was conducted to produce the DMN arrays with cavities caused by the shrinkage of the CMC solution. The resultant structures were detached from the mold.

Next, the arrays were positioned and fixed exactly in the holes of the fixing layer, and the protective layer with the same array of holes was assembled by aligning the holes for masking (Fig. 1B). After loading the FNS powder into the holes of the protective layer, the two layers were centrifuged to load the powder into the cavities of the DMNs. After de-masking the protective layer, a second protective layer with a thin CMC film was assembled to physically seal the open base part of FNS-PCMs to prevent the scattering of FNS powder. The micropillar arrays were then aligned with the holes of the second protective layer, resulting in the FNS-PCM implantation device.

3.2. Transdermal delivery of FNS-PCMs with DE

Fig. 2 shows a schematic illustration of the transdermal delivery of FNS-PCMs with a DE. Arrays of 5 × 5 FNS-PCMs were fabricated in a customized, micropillar-based implantation device, which enabled the microneedle arrays to be implanted in less than a second without any sticky-patches (Fig. 2A) [30]. After positioning of this device directly above the skin, the arrays of micropillars inside the device were pushed, resulting in full implantation of the FNS-PCM arrays (Fig. 2B). This complete implantation of FNS-PCMs made it possible to direct insert the FNS powder by using the inherent microneedle function of physically skin penetration, and thus DE could be applied sequentially on the implantation site of the FNS-PCMs (Fig. 2C). In addition, the FNS powder was located in the cavity of DMN structures and physically sealed using a thin CMC film, which enabled the powder to be implanted and remain under the dermis during DE application. As the DE diffused into the skin via the micro-channels created by the FNS-PCMs, the FNS powder was dissolved and then released into the dermal layer, resulting in intradermal FNS powder delivery.

3.3. Morphology, physical properties, and skin penetration analysis of FNS-PCMs

Before loading the FNS powder into the DMN arrays with cavities, their morphology was verified under an optical microscope to confirm the uniformity and specificity of each microneedle structure. The DMNs were fabricated based on a mold casting method; therefore, the height and base diameter of each structure were determined from the morphology of microneedle master structures as 801.5 ± 6.2 μm and 450.7 ± 6.8 μm, respectively (Fig. 3A, n = 4, mean ± SEM). In addition, the cavities for loading the FNS powder were formed in the center of the DMNs at a height of 426.7 ± 16.6 μm (dotted red line). In an image of the 5 × 5 arrays, the DMNs showed uniform and symmetric cone shapes with the regular cavities. Moreover, after loading the FNS

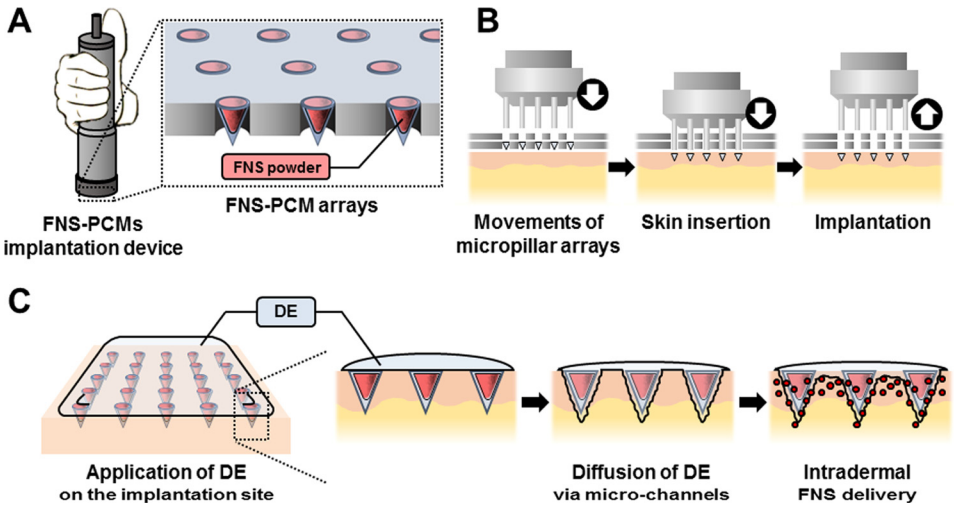

Fig. 2. Schematic representation of the finasteride (FNS)-loaded powder-carrying microneedles (FNS-PCMs) device and application with the diffusion enhancer (DE). (A) Arrays of 5 × 5 FNS-PCMs were housed in a micropillar-based implantation device. (B) Movement of the micropillar arrays toward the skin enabled full insertion of the FNS-PCMs, and retraction resulted in their implantation inside the skin. (C) Upon completion of implantation, DE was applied sequentially on the implantation site of the FNS-PCMs. Diffusion of DE via the microchannels enabled the FNS powder to be dissolved and then released into the dermal layer.

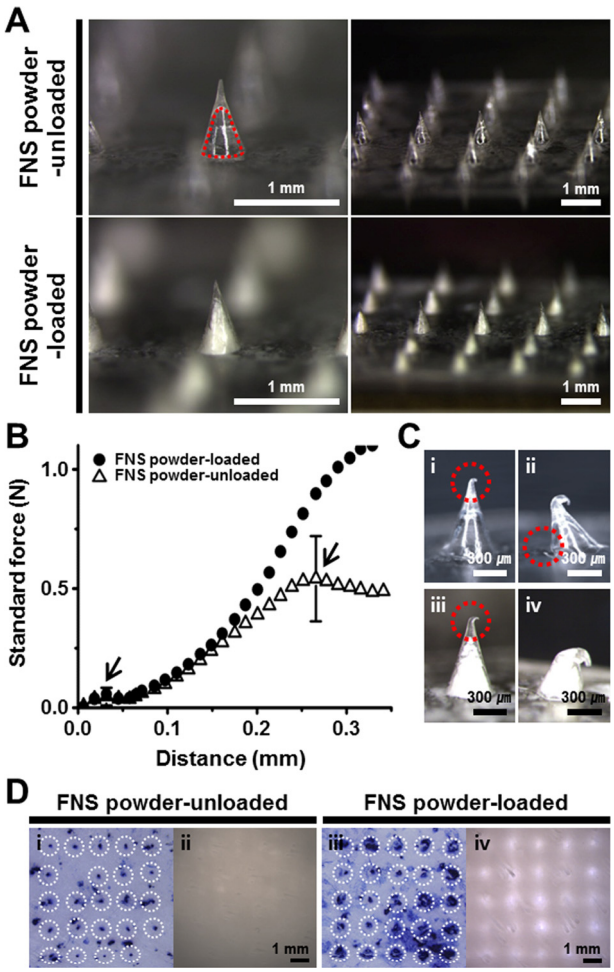

Fig. 3. (A) Microscopic images of single dissolving microneedle (DMN) and the arrays with cavities before and after loading of the finasteride (FNS) powder (Scale bar, 1 mm). The dotted red line indicates the cavity for loading the FNS powder. (B) Standard force of a single DMN structure before and after loading the FNS powder, which was recorded by moving the probe along the axial distance; the peaks of the graphs indicate the fracture force (arrows, n = 4, mean ± SEM). Both groups showed a first fracture when the tip part was broken, whereas additional fractures occurred at the base part only in FNS powder-unloaded group. (C) The FNS powder-unloaded group showed a fracture of the tip (i; dotted red circle) and a base fracture (ii) in microscopic images, while the FNS powder-loaded group showed only the tip fracture (iii) and the base fracture did not occur until 1 N of axial force was applied (iv, Scale bar: 300 μm). (D) In skin penetration analysis, the FNS powder-unloaded group showed imperfect skin perforation of both the outer surface (i; white dotted circles) and inner surface of the skin (ii), whereas the FNS powder-loaded group showed the 5 × 5 pattern of perforations in the outer surface (iii; dotted white circles) and inner surface (iv), indicating formation of the micro-channels caused by the FNS-PCM puncture (Scale bar, 1 mm).

powder, we observed that the FNS powder was fully filled into the center of the DMN cavity, which confirmed that the FNS powder was loaded directly into the DMN structures (i.e., FNS-PCMs). Conventional DMN techniques have mainly focused on hydrophilic compounds because of the water-soluble nature of backbone polymers; however, this result showed that PCM could encapsulate any powder formulations including lipophilic compounds, without considering the characteristics of the polymers. The arrays of FNS-PCMs also showed uniform shapes when encapsulating the FNS powder and contained a total of 209.8 ± 8.7 μg of FNS (n = 4, mean ± SEM).

The cavities of the DMN structures for loading FNS powder would decrease the mechanical strength of the structures and might fail to penetrate the skin [35]; therefore, a mechanical force was applied to confirm the skin penetration ability [31,32]. Representative graphs for the mechanical strength of the FNS powder-unloaded group (DMNs before loading the FNS powder) and the FNS powder-loaded group are shown in Fig. 3B (n = 4, mean ± SEM). As a result, the FNS powder-unloaded group showed two factures as the peaks of the graph, 0.062 ± 0.037 N at 30.3 ± 4.5 μm and 0.634 ± 0.179 N at 361.3 ± 9.3 μm, respectively (arrow marks). As a result, the FNS powder-unloaded group showed two factures as the peaks of the graph, 0.062 ± 0.037 N at 30.3 ± 4.5 μm and 0.634 ± 0.179 N at 361.3 ± 9.3 μm, respectively (arrow marks). Based on the distance values at which the fractures occurred, we could predict that the first fracture occurred when the tip part was broken, and the second fracture occurred in the structure itself. By contrast, the FNS powder-loaded group showed one fracture as 0.066 ± 0.011 N at 40.2 ± 9.4 μm, which was similar to the first fracture of the unloaded DMN structure, indicating that only the tip part was broken. Microscopic imaging confirmed that the FNS powder-unloaded group had two fractures at the tip of the structure (i), and at the base part (ii) (Fig. 3C, dotted red circles). However, FNS powder-loaded group showed a fracture only at the tip part (iii) and no additional fracture occurred during the test (iv), which suggested that loading the FNS powder in the cavity of DMN increased the mechanical strength of the base part of the structure by occupying the empty space.

In parallel, the FNS powder-unloaded group showed imperfect perforation of the pig cadaver skin (i; dotted white circles, Fig. 3D), which reconfirmed the decreased mechanical strength caused by the cavities in the DMN arrays. The underside (inner surface) of the skin also showed no changes compared with the intact skin (ii). By contrast, the FNS powder-loaded group showed a 5 × 5 pattern of perforations that exactly matched the FNS-PCM arrays (iii; dotted white circles), and the inner surface of the skin showed the same pattern, indicating formation of the micro-channels caused by FNS-PCM puncture (iv); this demonstrated that the FNS-PCMs were able to penetrate the skin, allowing delivery of the encapsulated FNS powder directly inside the skin.

3.4. Qualitative distribution analysis of Nile red-PCMs and gel

Although FNS powder was successfully implanted inside the skin by using the inherent microneedle function of physical penetration, the FNS powder could not be dissolved and diffused inside the skin due to its lipophilic and crystalline characteristics [26,27]; therefore, the implanted FNS powder after application of FNS-PCMs was expected to have no biological activity. Especially, FNS-gels contain formulations of organic solvents to deliver FNS topically, such as ethanol and propylene glycol, the former being reported to solubilize FNS, contributing to the formation of an elastic film on skin and/or hair surface and deposit the drug within the follicle, while the latter being known to act as a drug penetration enhancer, solvate keratin within the stratum corneum and the intercalate in the polar head groups of the lipid bilayers [13]. In these perspectives, an additional topical formulation, similar compositions to that of FNS-gel's solvents, would also be required to overcome these limitations and thus activate the biological functions of the implanted FNS powder inside the skin. We used Nile red as a model drug instead of FNS to confirm qualitative distribution analysis of this system because Nile red is a hydrophobic dye that is non-fluorescent in water or other polar solvents, but fluoresces when dissolved in an organic solvent [36]. The observations of Nile-red fluorescence indicated the dissolution and diffusion of Nile red powder inside the skin, which verified the need for the additional application of the DE on the FNS-PCMs implantation site. The distributions of Nile-red in the Nile red-PCM only and the Nile red-PCM/DE group were compared after removing the implanted residual Nile red powder inside the skin that remained in a powdered state, which was non-fluorescent and thus indicated no biological activity.

As a result, the Nile red-PCM only group showed no purple color at

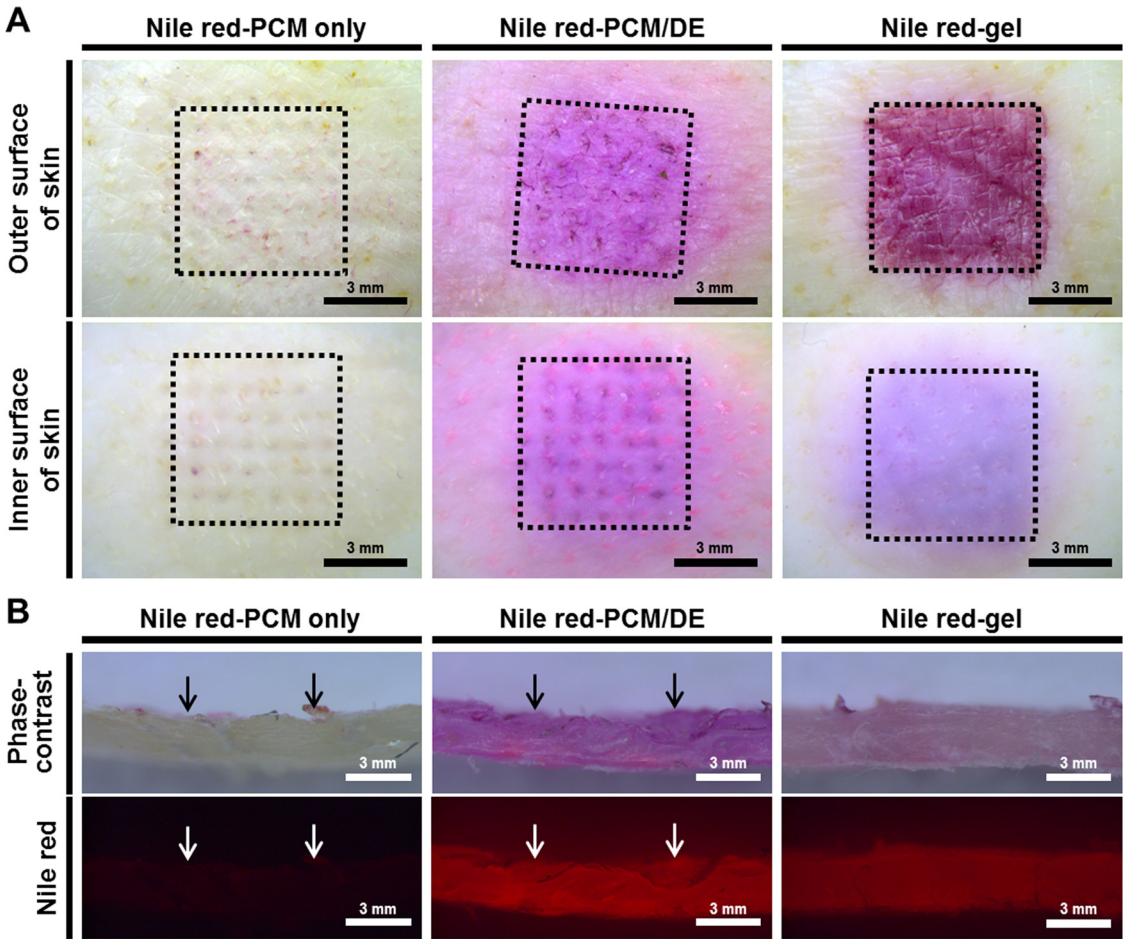

Fig. 4. (A) Distribution analysis after 24 h of permeation in the Nile red powder-loaded powder-carrying microneedle (Nile red-PCM) and Nile red-gel groups (Scale bar, 3 mm). The Nile red-PCM only group showed no purple color at the application site (1 cm^2, black dotted squares) in both the outer and inner skin surfaces, whereas the application of Nile red-PCM with the diffusion enhancer (DE) showed purple staining over the application site (Nile red-PCM/DE group); this indicated that the DE was necessary for lipophilic powder drug delivery and could facilitate the vertical diffusion of Nile red via the micro-channels. The Nile red-gel group showed more intense staining in the outer surface and less intense staining in the inner surface, indicating limited vertical diffusion of the gel formulation through the stratum corneum. (B) Cross-sectioned images demonstrated that diffusion of Nile red did not occur in the Nile-red PCM only group (Scale bar, 3 mm). Both Nile red-PCM/DE and Nile red-gel group showed vertical diffusion in the phase contrast and fluorescent images; however, the fluorescence intensity in the Nile red-PCM/DE group was higher than that in the gel group. Arrows represent the implantation sites of the Nile red-PCMs.

the application site (outer surface of the skin), representing the dissolution and diffusion of Nile red, even though successful skin penetration was demonstrated by the patterns of the microchannels in the inner surface of the skin (Fig. 4A). This indicated that all the Nile red powder was washed out and could not diffuse into the skin. By contrast, the Nile red-PCM/DE group showed the purple color over the application site (1 cm^2, black dotted squares), which demonstrated that the sequential application of the DE facilitated the lateral diffusion of Nile red encapsulated in the PCMs. In addition, in the images of the inner surface of the skin, both groups showed 5 × 5 patterns of perforations in the application area of 1 cm^2, reconfirming the successful penetration and micro-channel formation via the Nile red-PCMs, as shown in Fig. 3D. However, purple staining representing the diffusion of Nile red via the micro-channels under 800 μm (the thickness of the pig cadaver skin) was only observed in the Nile red-PCM/DE group, which indicated that DE application was required for lipophilic powder drug delivery and that it promoted the vertical diffusion of Nile red via the channels. The FNS powder has similar lipophilic characteristic to Nile red; therefore, these results suggested strongly that application of the DE on the implantation site of FNS-PCMs is a prerequisite for intradermal delivery of FNS. In the Nile red-gel group, purple staining was observed in both the outer and inner surfaces of the skin; however, the staining area was limited to the application site indicating limited lateral diffusion of Nile red compared with that observed for the Nile red-PCM/DE group. Moreover, the Nile red-gel group showed a more intense purple color on the outer surface of the skin and a less intense color on the inner surface, compared with that in the Nile red-PCM/DE group, indicating limited vertical diffusion of the gel formulation through stratum corneum. This result suggested that an application including FNS-PCMs with the DE could deliver FNS more effectively to the reticular and hypodermic regions compared with that of the FNS-gel formulation.

Cross-sectioned images of the skin in the Nile-red PCM only group, Nile-red PCM/DE group, and Nile red-gel group are shown in Fig. 4B. These results also demonstrated that diffusion of Nile red did not occur in the Nile-red PCM only group, whereas the Nile red-PCM/DE and Nile red-gel group showed vertical diffusion of Nile red throughout the skin on both phase contrast and fluorescent images. Moreover, in the Nile red-PCM/DE group, the fluorescence intensity was higher than that of the gel group, which confirmed that this application system is more effective to deliver FNS intradermally than the gel formulation.

3.5. In vitro skin permeation and retention of FNS

Next, instead of Nile red powder, FNS powder was loaded into the PCMs to quantitatively demonstrate the transdermal delivery of FNS via

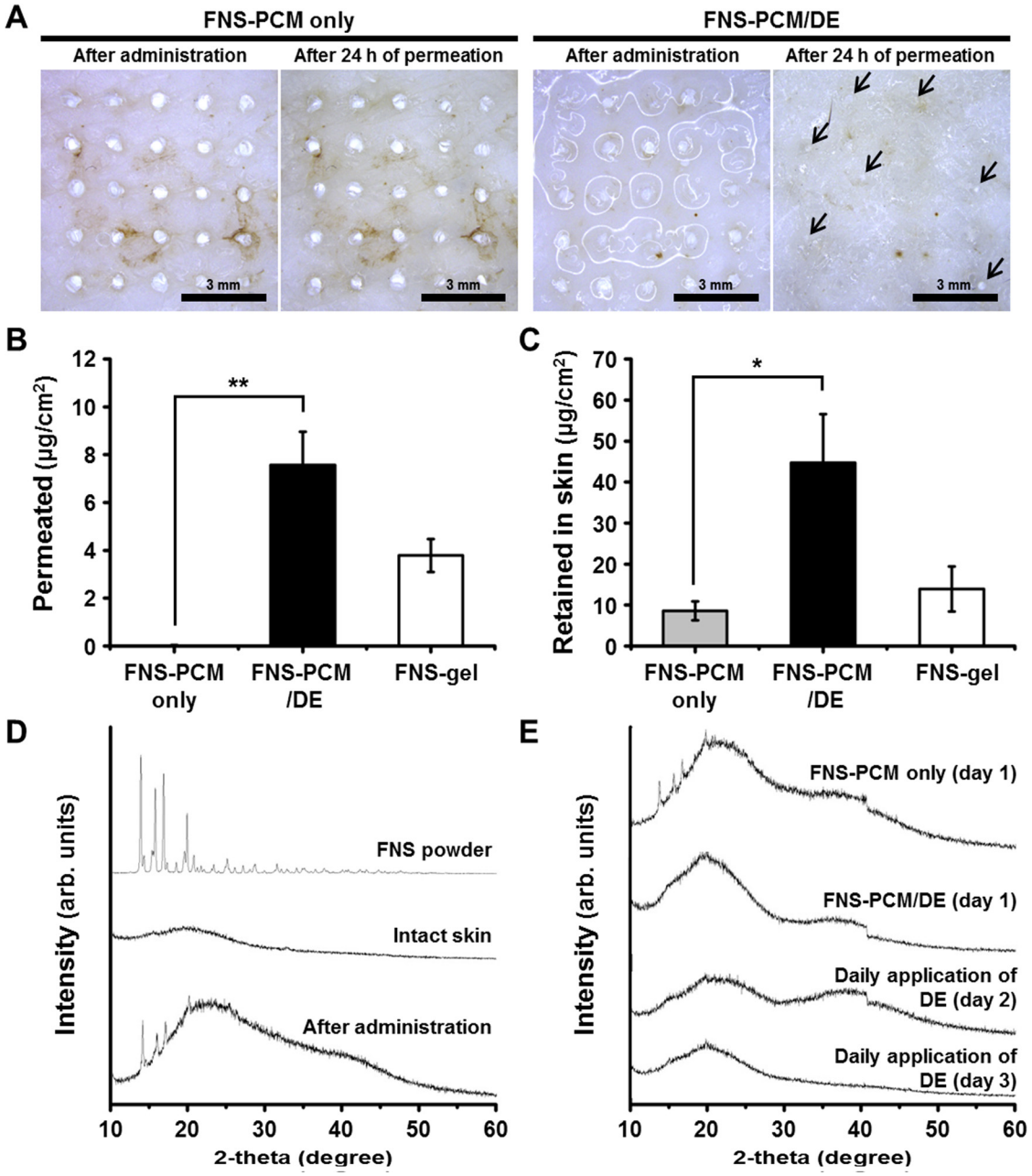

Fig. 5. (A) *In vitro* skin permeation test in finasteride (FNS)-loaded powder-carrying microneedles (FNS-PCMs) with the diffusion enhancer (DE). The FNS-PCM only group showed no differences in the white spots representing the crude FNS powder immediately after administration and after 24 h of permeation, which demonstrated that the FNS powder could not diffuse out after application of FNS-PCMs only. The spots in the FNS-PCM with DE group (FNS-PCM/DE) markedly disappeared after 24 h, with some residuals (arrows), indicating that DE application enabled the permeation of FNS inside the skin (Scale bar, 3 mm). Quantitative analysis of permeated (B) and retained (C) amounts of FNS after removing the implanted crude FNS powder (white spots) inside the skin (n = 4, mean ± SEM). The FNS-PCM/DE group showed higher amounts of permeated and retained FNS than the FNS-PCM only and FNS-gel groups (*$p < 0.05$ and **$p < 0.01$ compared with the FNS-PCM only group). X-ray diffraction (XRD) of FNS powder, intact skin, after administration of FNS-PCMs immediately (E) and FNS-PCM only, FNS-PCM/DE with daily application of DE (F) after the permeation test for the analysis of phase transitions and the diffusivity of FNS powder inside the skin.

PCM combined with DE application in a Franz diffusion cell test. Immediately after administration and at 24 h of permeation, there were no differences in the white spots at the implantation site of the FNS-PCMs in the FNS-PCM only group (Fig. 5A). The white spots indicated the FNS powder; therefore, this result implied that the FNS powder encapsulated in the FNS-PCMs remained at the site for 24 h without dissolution. This also confirmed that FNS powder could not diffuse out when applied as FNS-PCMs only, similar to the Nile red distribution pattern. In the FNS-PCM/DE group, however, these spots disappeared substantially after 24 h of permeation, although some residual white spots were observed inside the skin (arrow marks), indicating that DE application enabled the permeation of FNS inside the skin.

After the test, the amount of permeated FNS was sampled in the receptor fluid, and the powder that had not dissolved and diffused out by DE application, which remained inside the skin in a powdered state at the implantation sites (white spots), was washed out several times with distilled water. The amount of retained FNS, which diffused out and thus accumulated inside the skin, was measured using HPLC. In the quantitative analysis, the FNS-PCM only group showed 0.02 ± 0.02 μg and 8.60 ± 2.29 μg of permeated and retained FNS, respectively, which confirmed that most of the FNS powder encapsulated in the FNS-PCM arrays (209.8 μg) could not diffuse into the skin and was thus

washed out (Fig. 5B and C, n = 4, mean ± SEM). By contrast, the FNS-PCM/DE group showed 7.57 ± 1.39 μg ($p < 0.01$) and 44.70 ± 8.14 μg ($p < 0.05$) of permeated and retained FNS, respectively, which confirmed that the application of DE on the sites of FNS-PCMs is a prerequisite for the intradermal delivery of FNS. However, the sum of the permeated and retained amounts of FNS was only 52.27 μg in FNS-PCM/DE group, whereas the amount of FNS contained in FNS-PCM arrays was 209.8 ± 8.7 μg. The FNS-PCM/DE group also showed residual white spots representing crude FNS powder after 24 h of permeation; therefore, these implanted residuals might have been washed out and thus the sum of the permeated and retained FNS was lower than the original amount in the FNS-PCM array. Based on these results, the application of additional DE was expected to facilitate the diffusion of the residual implanted FNS powder. In the FNS-gel group, the permeated and retained amounts were lower than those in the FNS-PCM/DE group at 3.79 ± 0.69 μg and 13.93 ± 5.51 μg, respectively. The sum of the permeated and retained FNS in the gel group was only 17.72 μg, which also demonstrated that the novel application of FNS-PCMs with DE could deliver FNS 2.95 times more effectively than topically applied FNS by permeating the stratum corneum.

3.6. In vitro diffusivity analysis of FNS by XRD

The phase transition of FNS from crystal to amorphous inside the skin by DE is an important aspect of this system for confirming the diffusivity and permeation of FNS. Therefore, phase changes and diffusion of FNS were studied by XRD patterns of the skin samples after the permeation test. As shown in Fig. 5D, FNS powder exhibited a sharp intense Bragg's peak with narrow range scattering of X-rays at the angles of 13.92°, 15.78°, 16.86° and 19.9°, due to the crystalline nature of FNS, while intact skin showed broad humps without crystalline peaks scattering from a wide range of directions. However, after administration of FNS-PCMs inside the skin immediately, the intensity of peaks were increased at the angles approximately from 13.58° to 44.50° especially with the sharp peaks of FNS powder, confirming that the FNS powder was successfully implanted inside the skin without changing its phase transitions of crystalline nature.

After the 24-h permeation, FNS-PCM only group showed the same patterns to that of the skin after administration of FNS-PCMs immediately, which demonstrated that FNS powder preserved its crystalline nature and was not diffused inside the skin over the day (Fig. 5E). By contrast, FNS-PCM/DE group exhibited the decreased intensity compared to the FNS-PCM only group, confirming DE application enabled the permeation of FNS inside the skin. Moreover, with daily application of DE, the intensity of the crystalline nature of FNS-PCMs' implanted skin was decreased over the days (day 2 and day 3) and finally showed broad humps without crystalline peaks similar to that of the intact skin group. This demonstrated that the implanted FNS powder was changed to amorphous by application of DE, and diffused out over the days with daily application of DE using implanted FNS powder as a reservoir inside the skin.

3.7. Clearance of implanted FNS powder

For successful intradermal delivery of lipophilic FNS inside the skin, the application of additional DE on the implantation sites is a prerequisite. However, one application of DE could not achieve the complete delivery of the FNS encapsulated in the FNS-PCMs after 24 h of permeation and the crystallinity of FNS-PCMs' implanted sites were reduced gradually over the days with additional application of DE; therefore, we tested the appropriate number of applications of additional DE that could clear FNS powder, which would validate the safety of the procedure. Furthermore, for the cumulative application of FNS-PCMs, the number of additional DE applications was determined based on the clearance of the FNS retained inside the skin (n = 4 per group). As shown in Fig. 6A, white spots of FNS powder encapsulated in the FNS-PCMs were clearly visible at the implantation site (i), and after the immediate application of DE (ii). In parallel with the 24 h permeation data shown in Fig. 5A, these spots disappeared after 1 day, with some residual white spots representing the remaining FNS powder inside the skin (Fig. 6B, i), demonstrating that most of the implanted FNS powder was cleared. Moreover, with daily application of additional DE, the spots disappeared over subsequent days and were not observed after 3 days, indicating the complete clearance of the implanted FNS powder from the application sites (ii; day 2, iii; day 3).

In the quantitative analysis, the content of residual FNS in the mouse dorsal skin also decreased over time (Fig. 6C, mean ± SEM). On day 0, after the implantation of FNS-PCMs and the immediate sequential application of DE, the residual FNS was measured as 202.62 ± 9.01 μg, similar to that of encapsulated FNS in PCMs, which confirmed that almost 100 % of FNS was delivered in the skin successfully. In addition, the residual FNS content gradually decreased over time after the daily application of DE (day 1; 33.46 ± 23.11 μg, day 2; 3.59 ± 3.42 μg) and finally cleared after 3 days. This finding suggested that the FNS-PCM/DE system could continuously deliver FNS for 3 days with daily application of DE using implanted FNS powder as a reservoir inside the skin. In addition, 209.8 μg of FNS could be delivered intradermally via one application of FNS-PCMs, whereas the FNS-gel with daily application only delivered total 75 μg during the same period (calculated by daily application of 10 μL (25 μg) of FNS-gel at a concentration of 0.25 %, w/v). Although the DE was also applied daily to facilitate the diffusion of the implanted FNS powder inside the skin, the FNS-PCMs could deliver about 2.80 times more FNS on the same application area, exhibiting enhanced efficacy compared with that of the gel formulation. Moreover, for confirming the necessity of additional application of DE, we analyzed the residuals of FNS in the groups without DE application in the middle of the test as controls (day 1 without DE, and day 2 without DE group). Although the residuals of FNS in these groups were also decreased without DE application, the residuals were higher (day 1 without DE; 19.16 ± 10.73 μg, day 2 without DE; 0.62 ± 0.29 μg) compared to the results of the daily application of DE groups, confirming that additional application of DE facilitated diffusion of implanted FNS powder inside the skin. Based on these findings, the interval of FNS-PCMs application was set as 3 days with the daily application of DE for safe and effective FNS delivery. Also, the subsequent assessments were set as demonstrating the efficacy of FNS-PCM/DE group compared with control and FNS-gel group.

3.8. Evaluation of hair growth promotion

Using FNS-PCMs delivered at 3-day intervals with daily application of DE, the hair growth promotion of the FNS-PCM/DE group was compared with that of the FNS-gel and control group (n = 5 per group) reflecting simplified hair growth promotion in male mice model [10,34]. Representative images in each group following the test are shown in Fig. 7A. At the beginning of the test, there were no significant differences between the groups. However, based on visual scoring using the hair growth quantification scale [33,34], the FNS-PCM/DE group showed a slightly "grey to black coloration" status on day 3; and this reached "sparse long hair" on day 6 and "dense long hair" on day 9, which indicated significant promotion of hair growth compared with that of the FNS-gel and control group. Although the FNS-gel group showed slightly enhanced efficacy compared with the control group, the enhanced efficacy in the FNS-PCM/DE group revealed that the FNS powder was implanted successfully and delivered to hair follicles effectively via application of FNS-PCMs with DE. In parallel, the hair growth quantification score in the FNS-PCM/DE group was higher than that of the FNS-gel and control group during the whole course of the test (Fig. 7B, mean ± SEM). There were no differences between the groups up to 3 days; however, the FNS-PCM/DE group showed significant hair growth scores at 6 days ($p < 0.05$) and 9 days ($p < 0.01$), which suggested that this novel application system facilitated

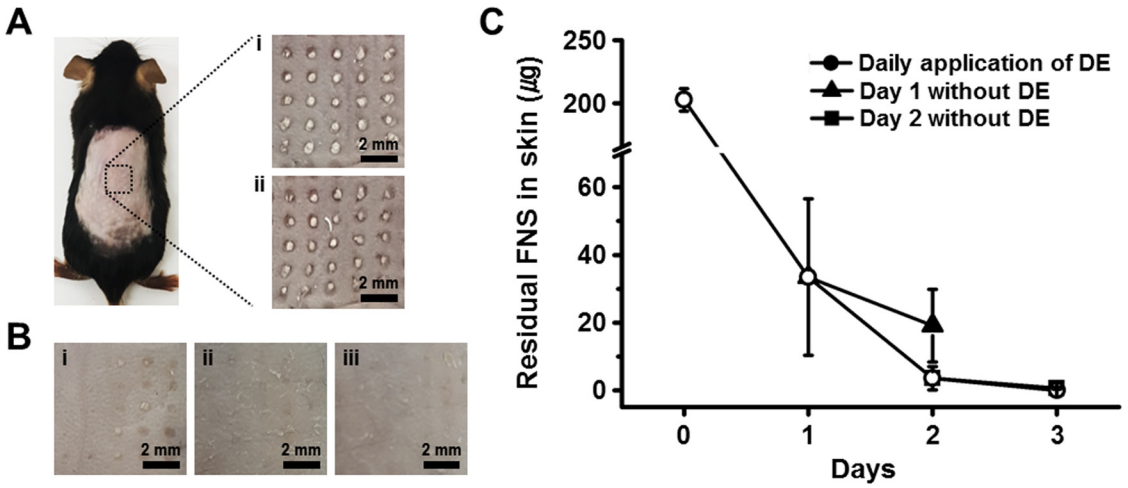

Fig. 6. (A) Images of the dorsal skin of a mouse showing the implantation site of finasteride (FNS)-loaded powder-carrying microneedles (FNS-PCMs) with sequential application of diffusion enhancer (DE). Immediately after implantation, white spots of FNS powder were clearly visible at the implantation site (i), and after the application of DE (ii; Scale bar, 2 mm). (B) With daily application of DE, the spots disappeared after 1 day, with some residuals (i) and almost completely disappeared over subsequent days (ii; day 2, iii; day 3). (C) The residual FNS content decreased over time and finally cleared after 3 days, confirming that the suitable interval of FNS-PCM treatment with daily application of DE was 3 days (n = 4, mean ± SEM).

faster hair growth than the FNS-gel or control group (images of the hair growth status in all groups are shown in Supplementary Fig. 1). Moreover, as FNS-PCMs could be implanted inside the skin and be diffused by DE over the days; this indicated that FNS-PCM/DE system could deliver FNS more efficiently than topical gel formulations. Since the topical FNS-gel could not be efficiently diffused out intradermally as shown in Fig. 5B and C, this demonstrated that FNS could be washed out by sweat or daily hair washing with loss of the active compound, FNS. FNS-PCM/DE system was also considered to prohibit daily exercise or hair washing after immediate application of FNS-PCM, since the time for skin resealing by microneedle punctuation are 10–12 h [37]. After administration, however, the polymer matrix, CMC, was dissolved out by DE and skin interstitial fluid, and thus FNS powder remained implanted inside the skin by the skin resealing process. This

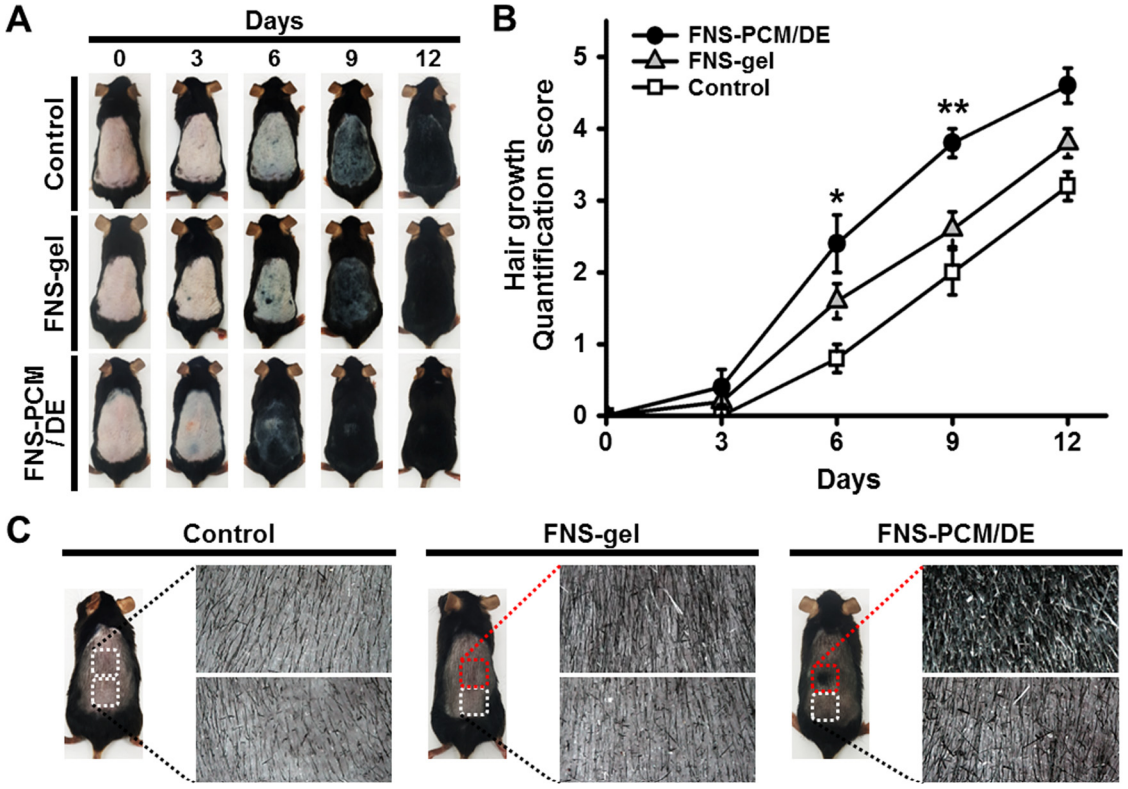

Fig. 7. (A) Images of representative mouse hair growth status in the non-treated group (control), in the daily application of finasteride-gel group (FNS-gel), and in the group receiving 3-day intervals of FNS-loaded powder-carrying microneedles (FNS-PCMs) with daily application of diffusion enhancer (DE) (FNS-PCM/DE). (B) Hair growth quantification score during the whole course of the test (n = 5, mean ± SEM, $*p < 0.05$ and $**p < 0.01$ for the FNS-PCM/DE group *vs.* the control group). (C) Images of the application sites (red dotted squares) and non-treated sites (white dotted squares) 1 week after the test. The FNS-PCM/DE group showed a significant mass of dense hair over the application area, confirming the efficacy of the treatment for hair growth, as well as increasing the amount and density of the hair.

indicated that this system could overcome the limitations of daily hair washing without loss of FNS after skin resealing. Moreover, during the 2 days of clearance, FNS powder remained inside the fully-resealed skin indicating this FNS-PCM/DE system could be utilized as a practical delivery system without loss of FNS by overcoming sweat or daily hair washing.

In particular, in the FNS-PCM/DE group, the hair on the FNS-PCM application sites remained at the "sparse long hair" status, and was not fully grown, which might have been caused by the micro-wounds resulting from the cumulative application of FNS-PCMs (Supplementary Fig. 2). Since this FNS-PCM/DE system was based the inherent microneedle function which overcomes the skin barrier properties physically, this indicated that frequent usage of FNS-PCMs could result in damages on scalp by FNS-PCMs' punctures. However, at 1 week after the test, the hair on the application sites became similar to that of the surrounding scalp, which indicated restoration of fully-grown hair at the application sites reveals the reversible skin restoring by this system considered as safe without frequent usage and could be utilized for male androgenetic alopecia.

Furthermore, the dorsal skin of all groups was shaved using an electric clipper 1 week after the test, and the application sites (red dotted squares) and non-treated sites (white dotted squares) were analyzed (Fig. 7C). Compared with that of the control group, the FNS-gel group showed an area of slightly dense hair on the application site, indicating the efficacy of the FNS-gel. In the FNS-PCM/DE group, however, the application site showed a significant mass of dense hair with the area of 1.11 ± 0.24 cm^2, which was larger than that of the application area of the FNS-PCMs (images of shaved dorsal skin in all groups are shown in Supplementary Fig. 3). Since the non-treated sites for FNS-PCM/DE group were not significantly different compared to control and FNS-gel group, we determined that FNS-PCM/DE system had no systemic effect and FNS was delivered locally on the application area of FNS-PCMs. Further, we plan to study the system exposure of this system compared to other different dosage forms, oral FNS and topical FNS-gel. Also, the study related to inhibition of DHT in hair follicles and androgen dependent tissue is planned in future. In conclusion, in terms of efficacy, the application of FNS-PCMs with a DE could deliver FNS to hair follicles effectively, which facilitated hair growth, as well as increased amounts and density of the hair.

3.9. Storage stability test

The amount of FNS in all formulations (dry powder, gel, and PCMs) stored at 25 °C was evaluated over 8 weeks. FNS is a synthetic compound and is stable at room temperature; the amount of FNS was maintained at more than 97 % in all groups over 8 weeks of storage (Supplementary Table 1, n = 4, mean ± SEM). This result demonstrated that FNS encapsulated in PCMs was stable, which would permit their wide use as a platform for a lipophilic drug-delivery comprising long-term stability with no apparent safety issues.

4. Conclusion

This study revealed a novel intradermal FNS powder delivery system combined with DE for the effective treatment of androgenetic alopecia. The system overcomes the limitations of conventional DMN techniques by encapsulating FNS powder using PCMs, and the application of the DE on the implantation site of the FNS powder enabled enhanced transdermal delivery of FNS. Compared with the gel formulation, this novel system showed effective *in vivo* efficacy, in terms of hair growth promotion, the amount and density of the hair, with satisfactory safety. This approach has the potential to advance the field of transdermal drug delivery via its ability to deliver any type of powdered drug for a wide variety of biomedical applications.

Declaration of Competing Interest

Hyungil Jung has submitted patents that have been or may be licensed to Juvic Inc. and is a founder/shareholder of Juvic Inc., developing microneedle-based products. These potential conflicts of interest have been disclosed and are being managed by Yonsei University.

Acknowledgements

This work was supported by the Technology Development Program (S2641709) funded by the Ministry of SMEs and Startups (MSS, Korea).

Appendix A. Supplementary data

Supplementary material related to this article can be found, in the online version, at doi:https://doi.org/10.1016/j.jconrel.2019.11.002.

References

[1] A.C. Heath, D.R. Nyholt, N.A. Gillespie, N.G. Martin, Genetic basis of male pattern baldness, J. Invest. Dermatol. 121 (2003) 1561–1564, https://doi.org/10.1111/j.1523-1747.2003.12615.x.
[2] J.A. Ellis, R. Sinclair, S.B. Harrap, Androgenetic alopecia: pathogenesis and potential for therapy, Expert Rev. Mol. Med. 4 (2002) 1–11, https://doi.org/10.1017/S1462399402005112.
[3] D. Stough, K. Stenn, R. Haber, W.M. Parsley, J.E. Vogel, D.A. Whiting, K. Washenik, Psychological effect, pathophysiology, and management of androgenetic alopecia in men, Mayo Clin. Proc. 80 (2005) 1316–1332, https://doi.org/10.4065/80.10.1316.
[4] K.J. McClellan, A. Markham, Finasteride: a review of its use in male pattern hair loss, Drugs 57 (1999) 111–126, https://doi.org/10.2165/00003495-199957010-00014.
[5] J.F. Libecco, W.F. Bergfeld, Finasteride in the treatment of alopecia, Expert Opin. Pharmacother. 5 (2004) 933–940, https://doi.org/10.1517/14656566.5.4.933.
[6] M. Tabbakhian, N. Tavakoli, M.R. Jaafari, S. Daneshamouz, Enhancement of follicular delivery of finasteride by liposomes and niosomes: 1. In vitro permeation and in vivo deposition studies using hamster flank and ear models, Int. J. Pharm. 323 (2006) 1–10, https://doi.org/10.1016/j.ijpharm.2006.05.041.
[7] A. Saraswat, B. Kumar, Minoxidil vs Finasteride in the treatment of men with androgenetic alopecia, Arch. Dermatol. 139 (2003) 1219–1221, https://doi.org/10.1001/archderm.139.9.1219-b.
[8] K.A. Gordon, A. Tosti, Alopecia: evaluation and treatment, Clin. Cosmet. Investig. Dermatol. 4 (2011) 101–106, https://doi.org/10.2147/CCID.S10182.
[9] R. Kumar, B. Singh, G. Bakshi, O.P. Katare, Development of liposomal systems of finasteride for topical applications: design, characterization, and in vitro evaluation, Pharm. Dev. Technol. 12 (2007) 591–601, https://doi.org/10.1080/10837450701481181.
[10] S.I. Lee, S.K.N. Sriraman, S. Shanmugam, R. Baskaran, C.S. Yong, S.K. Yoon, H.G. Choi, B.K. Yoo, Effect of charge carrier lipid on skin penetration, retention, and hair growth of topically applied finasteride-containing liposomes, Biomol. Ther. 19 (2011) 231–236, https://doi.org/10.4062/biomolther.2011.19.2.231.
[11] Y. Javadzadeh, J. Shokri, S.H. Nezhadi, H. Hamishehkar, A. Nokhodchi, Enhancement of percutaneous absorption of finasteride by cosolvents, cosurfactant and surfactants, Pharm. Dev. Technol. 15 (2010) 619–625, https://doi.org/10.3109/10837450903397610.
[12] T. Madheswaran, R. Baskaran, R.K. Thapa, J.Y. Rhyu, H.Y. Choi, J.O. Kim, C.S. Yong, B.K. Yoo, Design and in vitro evaluation of finasteride-loaded liquid crystalline nanoparticles for topical delivery, AAPS PharmSciTech 14 (2013) 45–52, https://doi.org/10.1208/s12249-012-9888-y.
[13] D. Monti, S. Tampucci, S. Burgalassi, P. Chetoni, C. Lenzi, A. Pirone, F. Mailland, Topical formulations containing finasteride. Part I: in vitro permeation/penetration study and in vivo pharmacokinetics in hairless rat, J. Pharm. Sci. 103 (2014) 2307–2314, https://doi.org/10.1002/jps.24028.
[14] R. Dhurat, S. Mathapati, Response to microneedling treatment in men with androgenetic alopecia who failed to respond to conventional therapy, Indian J. Dermatol. 60 (2015) 260–263, https://doi.org/10.4103/0019-5154.156361.
[15] R.M. Fertig, A.C. Gamret, J. Cervantes, A. Tosti, Microneedling for the treatment of hair loss? J. Eur. Acad. Dermatol. Venereol. 32 (2018) 564–569, https://doi.org/10.1111/jdv.14722.
[16] N. Wilke, A. Mulcahy, S.R. Ye, A. Morrissey, Process optimization and characterization of silicon microneedles fabricated by wet etch technology, Microelectron. J. 36 (2005) 650–656, https://doi.org/10.1016/j.mejo.2005.04.044.
[17] T. Omatsu, K. Chujo, K. Miyamoto, M. Okida, K. Nakamura, N. Aoki, R. Morita, Metal microneedle fabrication using twisted light with spin, Opt. Express 18 (2010) 17967–17973, https://doi.org/10.1364/OE.18.017967.
[18] S. Memon, D.N. Pathan, A.R. Ziyaurrahman, A. Bagwan, B. Sayed, Microneedle as a novel drug delivery system: a review, Int. Res. J. Pharm. 2 (2011) 72–77.
[19] X. Jin, D.D. Zhu, B.Z. Chen, M. Ashfaq, X.D. Guo, Insulin delivery systems combined with microneedle technology, Adv. Drug Deliv. Rev. 127 (2018) 119–137, https://doi.org/10.1016/j.addr.2018.03.011.
[20] K.M. Kwon, S.M. Lim, S. Choi, D.H. Kim, H.E. Jin, G. Jee, K.J. Hong, J.Y. Kim,

Microneedles: quick and easy delivery methods of vaccines, Clin. Exp. Vaccine Res. 6 (2017) 156–159, https://doi.org/10.7774/cevr.2017.6.2.156.
[21] M.R. Prausnitz, R. Langer, Transdermal drug delivery, Nat. Biotechnol. 26 (2008) 1261–1268, https://doi.org/10.1038/nbt.1504.
[22] K. Ita, Transdermal delivery of drugs with microneedles—potential and challenges, Pharmaceutics 7 (2015) 90–105, https://doi.org/10.3390/pharmaceutics7030090.
[23] K.Y. Seong, M.S. Seo, D.Y. Hwang, E.D. O'Cearbhaill, S. Sreenan, J.M. Karp, S.Y. Yang, A self-adherent, bullet-shaped microneedle patch for controlled transdermal delivery of insulin, J. Control. Release 265 (2017) 48–56, https://doi.org/10.1016/j.jconrel.2017.03.041.
[24] L.K. Vora, R.F. Donnelly, E. Larrañeta, P. González-Vázquez, R.R.S. Thakur, P.R. Vavia, Novel bilayer dissolving microneedle arrays with concentrated PLGA nano-microparticles for targeted intradermal delivery: Proof of concept, J. Control. Release 265 (2017) 93–101, https://doi.org/10.1016/j.jconrel.2017.10.005.
[25] H. Yang, S. Kim, M. Jang, H. Kim, S. Lee, Y. Kim, Y.A. Eom, G. Kang, L. Chiang, J.H. Baek, J.H. Ryu, Y.E. Lee, J. Koh, H. Jung, Two-phase delivery using a horse oil and adenosine-loaded dissolving microneedle patch for skin barrier restoration, moisturization, and wrinkle improvement, J. Cosmet. Dermatol. 18 (2019) 936–943, https://doi.org/10.1111/jocd.12768.
[26] M. Dangol, H. Yang, C.G. Li, S.F. Lahiji, S. Kim, Y. Ma, H. Jung, Innovative polymeric system (IPS) for solvent-free lipophilic drug transdermal delivery via dissolving microneedles, J. Control. Release 223 (2016) 118–125, https://doi.org/10.1016/j.jconrel.2015.12.038.
[27] J.U.A. Junghanns, R.H. Müller, Nanocrystal technology, drug delivery and clinical applications, Int. J. Nanomed. 3 (2008) 295–309.
[28] F. Chen, Q. Yan, Y. Yu, M.X. Wu, BCG vaccine powder-laden and dissolvable microneedle arrays for lesion-free vaccination, J. Control. Release 255 (2017) 36–44, https://doi.org/10.1016/j.jconrel.2017.03.397.
[29] M.T. Ghannam, M.N. Esmail, Rheological properties of carboxymethyl cellulose, J. Appl. Polym. Sci. 64 (1997) 289–301, https://doi.org/10.1007/s00396-008-1882-2.
[30] S.F. Lahiji, M. Dangol, H. Jung, A patchless dissolving microneedle delivery system enabling rapid and efficient transdermal drug delivery, Sci. Rep. 5 (2015) 7914, https://doi.org/10.1038/srep07914.
[31] S. Kim, M. Dangol, G. Kang, S.F. Lahiji, H. Yang, M. Jang, Y. Ma, C. Li, S.G. Lee, C.H. Kim, Y.W. Choi, S.J. Kim, J.H. Ryu, J.H. Baek, J. Koh, H. Jung, Enhanced transdermal delivery by combined application of dissolving microneedle patch on serum-treated skin, Mol. Pharm. 14 (2017) 2024–2031, https://doi.org/10.1021/acs.molpharmaceut.7b00111.
[32] S. Kim, J. Lee, F.L. Shayan, S. Kim, I. Huh, Y. Ma, H. Yang, G. Kang, H. Jung, Physicochemical study of ascorbic acid 2-glucoside loaded hyaluronic acid dissolving microneedles irradiated by electron beam and gamma ray, Carbohydr. Polym. 180 (2018) 297–303, https://doi.org/10.1016/j.carbpol.2017.10.044.
[33] C.H. Chen, M.T. Sheu, A.B. Wu, K.P. Lin, H.O. Ho, Simultaneous effects of tocopheryl polyethylene glycol succinate (TPGS) on local hair growth promotion and systemic absorption of topically applied minoxidil in a mouse model, Int. J. Pharm. 306 (2005) 91–98, https://doi.org/10.1016/j.ijpharm.2005.09.005.
[34] S. Shanmugam, R. Baskaran, S. Nagayya-Sriraman, C.S. Yong, H.G. Choi, J.S. Woo, B.K. Yoo, The effect of methylsulfonylmethane on hair growth promotion of magnesium ascorbyl phosphate for the treatment of alopecia, Biomol. Ther. 17 (2009) 241–248, https://doi.org/10.4062/biomolther.2009.17.3.241.
[35] Q.L. Wang, D.D. Zhu, X.B. Liu, B.Z. Chen, X.D. Guo, Microneedles with controlled bubble sizes and drug distributions for efficient transdermal drug delivery, Sci. Rep. 6 (2016) 38755, https://doi.org/10.1038/srep38755.
[36] I.R. Sitepu, L. Ignatia, A.K. Franz, D.M. Wong, S.A. Faulina, M. Tsui, A. Kanti, K. Boundy-Mills, An improved high-throughput Nile red fluorescence assay for estimating intracellular lipids in a variety of yeast species, J. Microbiol. Methods 91 (2012) 321–328, https://doi.org/10.1016/j.mimet.2012.09.001.
[37] Z. Zhu, H. Luo, W. Lu, H. Luan, Y. Wu, J. Luo, Y. Wang, J. Pi, C.Y. Lim, H. Wang, Rapidly dissolvable microneedle patches for transdermal delivery of exenatide, Pharm. Res. 31 (2014) 3348–3360, https://doi.org/10.1007/s11095-014-1424-1.